PERGAMON

International Journal of Solids and Structures 39 (2002) 1003–1014

INTERNATIONAL JOURNAL OF SOLIDS and STRUCTURES

www.elsevier.com/locate/ijsolstr

An analytical estimate of thermal effects in a composite bonded repair: plane stress analysis

C.N. Duong *, J. Yu

The Boeing Company, 2401 E. Wardlow Road, MC C078-0209, Long Beach, CA 90807-5309, USA

Received 12 October 2000

Abstract

The thermal effects due to curing of the adhesive and due to the low uniform operating temperature on crack patching efficiency in a composite bonded repair are estimated using a two-stage analysis procedure originally proposed by Rose (Int. J. Solids Struct. 17 (1981) 827). The problem is formulated for a bonded repair with an octagonal shaped patch by using the linear elasticity theory. The thermal stresses due to thermal expansion mismatch between the repaired skin and the patch are determined first as if the patch is bonded rigidly to an *uncracked* skin, by using the equivalent inclusion method. The stress intensity factor associated with these thermal stresses is then estimated by using the displacement compatibility method for a sandwich plate with a part-through and a debonding crack. © 2002 Elsevier Science Ltd. All rights reserved.

Keywords: Composite bonded repair; Thermal stresses; Stress intensity factor

1. Introduction

The efficiency of the repair technique involving adhesively bonded composite patch to increase the durability and damage tolerance of cracked aerospace metallic structures at low cost has been long recognized. Theoretical analyses to compute the stress intensity factor after repair had been conducted for both mechanical and thermal loadings (Rose, 1988; Freddell, 1994; Wang et al., 2000). However, these analyses were limited to a case of an elliptical or circular patch. Recently, Duong et al. (2001) had derived an approximate algorithmic solution for the elastic fields in an infinite isotropic sheet containing a rigidly bonded orthotropic patch of an octagonal shape subjected to a far field tension. As a continuing effort of that earlier work, the solution approach employed there will be extended here to include the analysis of a bonded repair under thermal loading.

Repaired structures are usually subjected to two types of thermal loading: heating and cooling cycle associated with the curing process of the adhesive and the low operating temperature of the aircraft during high altitude cruising. Since the thermal expansion coefficients of the repaired skin and the patch are

* Corresponding author. Tel.: +1-562-593-1421; fax: +1-562-982-7367.
E-mail address: cong.n.duong@boeing.com (C.N. Duong).

PII: S0020-7683(01)00239-6

significantly different, these thermal loads may induce large residually thermal stresses and therefore affect the efficiency of the repair. The objective of this study is, therefore, to develop an analytical method to characterize these thermal stresses and to estimate their effects on a cracked metallic skin repaired with an adhesively bonded composite patch. Even though the adhesive during bond formation is better characterized by a constitutive description which incorporates its dependence on the rate of mechanical deformation and on the thermal history (Duong and Knauss, 1995); however, for simplicity, the adhesive is modeled here as a linear elastic material with a zero stiffness and a glassy modulus at temperatures above and below its glass transition temperature, respectively.

2. Two-stage analysis procedure

The analysis of a bonded repair under thermal loading is divided into two stages as shown in Fig. 1, following Rose's approach. The value of dividing the analysis into these two stages is that each stage can be solved by a different analytical method employing different set of appropriate simplifying assumptions. In the first stage, the bond between the patch and the repaired skin is assumed to be rigid and the bonded structure is subjected to a thermal field simulating the curing process and the low operating temperature condition. The repaired skin is also assumed to contain no crack. This problem is solved by using the equivalent inclusion method, following the approach recently developed by Duong et al. (2001) for analyzing the stress field in an infinite isotropic sheet rigidly bonded with a polygon-shaped orthotropic patch under a far field tension. The thermal stresses at the prospective crack location are then determined. The effects of the thermally induced stresses on crack patching efficiency is then assessed in the second stage analysis, where a crack is introduced into a residually stressed, patched skin while the patch is assumed to be infinite extent. By employing the displacement compatibility method considered by Duong and Yu (1997) earlier for a part-through cracked sandwich plate, which accounts for both the pre-existing disbond around the crack and the flexibility of the adhesive, the stress intensity factor associated with these thermal stresses is finally estimated.

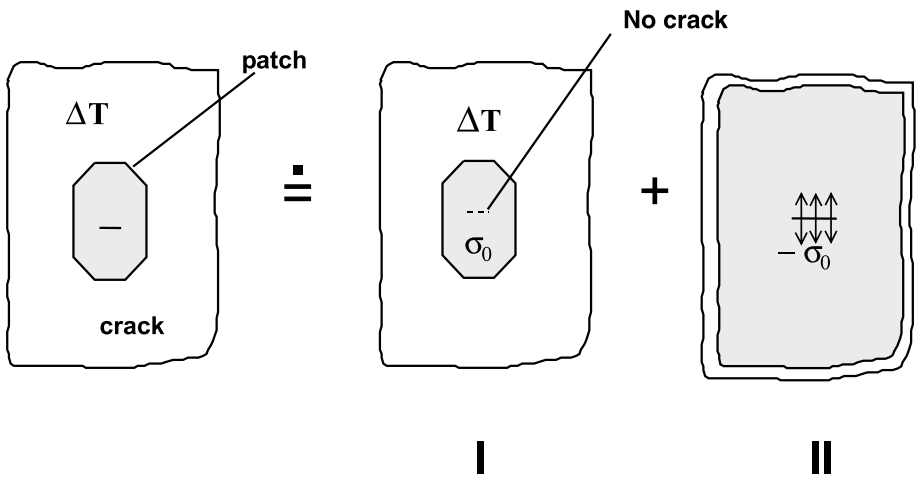

Fig. 1. Two-stage analysis in Rose's approach: (I) an uncracked skin containing an inhomogeneity under thermal loading, and (II) a part-through cracked sandwich plate under surface crack pressure.

3. Analytical solution

3.1. Stage I analysis

We will show first that the present thermal stress problem can be reformulated as an initial strain problem, in which the patch is subjected to a prescribed initial strain field. This way will allow us to solve the thermal stress problem directly within the context of the equivalent inclusion method. The equivalent initial strain field prescribed in the patch will be derived here for two cases: (a) thermal cycle associated with adhesive curing and (b) a uniform low operating temperature.

(a) Thermal cycle associated with adhesive curing: Adhesive curing usually involves heating the reinforced region using a heating blanket to a high temperature above the adhesive glass transition temperature under pressure for a few hours and then allowing the adhesive and adherends to cool to the ambient temperature. For simplicity, the temperature distribution around the heating blanket is assumed to be a step function with the inside region held at one constant temperature while the outside being at a constant ambient temperature. This assumption for the temperature field may not be realistic due to the heat conduction; nevertheless, the analysis considered here still can provide a first ordered estimate of the effect of curing on crack patching efficiency in the preliminary design phase. The effect of non-uniform thermal field has been addressed before by Rose (1988) and more recently by Wang et al. (2000) for a circular patch, which results can be used as correction factors for the present analyses.

During heating, the adhesive is assumed to be very soft so that the patch undergoes a free expansion while the skin is under thermal stresses because the skin material outside of the heating region is still cool. The thermal stresses in the skin during the heating phase can be easily calculated by using the Rodin's or Duong et al.'s solution for a polygon-shaped inclusion with a constant eigenstrain $\alpha_0\Delta T(\Delta T > 0)$, where α_0 is the skin thermal expansion coefficient and ΔT is the change in temperatures. The skin's total strain inside the heating region associated with these thermal stresses then can be calculated, which is smaller than $\alpha_0\Delta T$ and will be denoted here by $\varepsilon_{ij}^{(0)}$.

The next step is to cool the whole repair down to the ambient temperature. This cooling step will be divided further into two substeps: (i) the patch is first held at a constant curing temperature and simultaneously subjected to a fictitious initial strain field $-\varepsilon_{ij}^{(0)}$ while the skin is cooled, and (ii) the patch is then allowed to cool and to relax simultaneously the fictitious initial strain $-\varepsilon_{ij}^{(0)}$ imposed in (i). Since the patch is subjected to an initial strain $-\varepsilon_{ij}^{(0)}$ in substep (i), the skin will contract back to its original shape without experiencing any exerted forces from the patch, resulting in a stress free skin at the end of substep (i). It is then clear that the described thermal stress problem is now reduced to an initial strain problem with an initial strain of $-\alpha_{ij}^{\mathrm{p}}\Delta T + \varepsilon_{ij}^{(0)}$ prescribed in the patch, where again $\Delta T > 0$.

(b) Uniform low operating temperature: In this case, the whole patched skin is cooled uniformly. Following the same procedure as in (a), the skin is cooled uniformly first to a low operating temperature while the patch is still at the ambient temperature and is subjected to a fictitious initial strain field $\alpha_0\Delta T$, where α_0 and ΔT are already defined previously but $\Delta T < 0$ in the present case. This process will not result in any thermal stresses in the skin since the patch will not exert any force on the skin. The patch is then allowed to cool and to relax simultaneously the fictitious initial strain $\alpha_0\Delta T$ imposed previously. This thermal stress problem is again reduced to an initial strain problem with an initial strain of $(\alpha_{ij}^{\mathrm{p}} - \alpha_0)\Delta T$ prescribed in the patch.

With the equivalent initial strain prescribed in the patch already determined, we now proceed to the formulation of the mathematical model for stage I analysis. Since the patch is assumed to bond rigidly to a repaired skin over an octagonal region Ω, the patch is considered as an integral part of the skin inside Ω, and the skin with a patch incorporated is modeled as an inhomogeinity. This inhomogeinity has an effective stiffness C_{ijkl}^{I} and with a prescribed initial strain field $\varepsilon_{ij}^{(\mathrm{T})}$ as given in Appendix A. Let us therefore consider a problem of an infinite isotropic, linear elastic sheet (skin) with a stiffness C_{ijkl}^{0} containing an octagonal

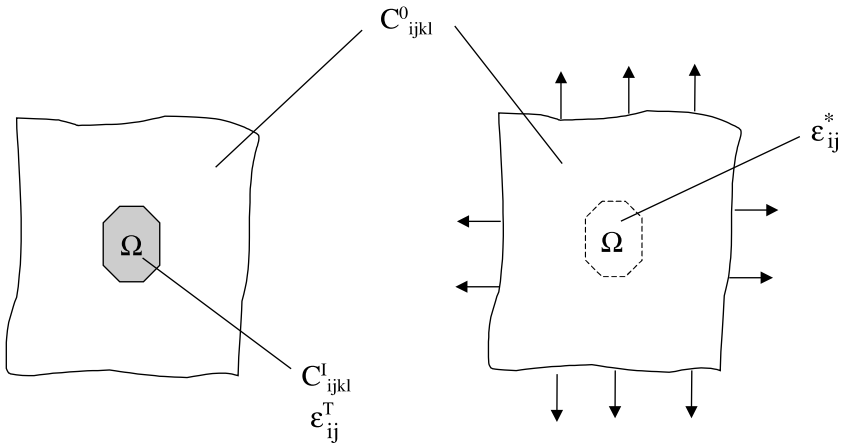

Fig. 2. An illustration of the equivalent inclusion method: (A) an inhomogeinity problem with a prescribed initial strain field ε_{ij}^{T}, and (B) an inclusion problem with eigenstrain ε_{ij}^{*}.

shaped inhomogeinity Ω with a stiffness C_{ijkl}^{I} and subjected to an initial strain field $\varepsilon_{ij}^{(T)}$. This problem will then be solved by the equivalent inclusion method outlined below.

In the equivalent inclusion method, the stress and strain fields induced by an inhomogeneity occupied region Ω will be the same as those induced by the eigenstrain field ε_{ij}^{*} in the same region of a homogeneous material C_{ijkl}^{0} when ε_{ij}^{*} is selected appropriately as shown in Fig. 2. Following the procedure given in (Duong et al., 2001) for an inhomogeneity symmetric with respect to both coordinate axes, by approximating ε_{ij}^{*} as a second ordered polynomials of the position coordinates with yet to be determined coefficients, i.e.,

$$\varepsilon_{ij}^{*} = B_{ij} + B_{ijkl}x_k x_l, \tag{1}$$

and by expanding the prescribed initial strain field $\varepsilon_{ij}^{(T)}$ into a Taylor series, the equivalency condition requires that B_{ij} and B_{ijkl} must satisfy the following system of linear equations (without summation on subscript α):

$$\begin{aligned}
&\Delta C_{\alpha\alpha 11}L_{11}(\mathbf{0}) + \Delta C_{\alpha\alpha 22}L_{22}(\mathbf{0}) - C_{\alpha\alpha 11}^{0}B'_{11} - C_{\alpha\alpha 22}^{0}B'_{22} = -C_{\alpha\alpha 11}^{I}\varepsilon_{110}^{(T)} - C_{\alpha\alpha 22}^{I}\varepsilon_{220}^{(T)};\\
&\frac{1}{2}\Delta C_{\alpha\alpha 11}\frac{\partial^2}{\partial x_1^2}L_{11}(\mathbf{0}) + \frac{1}{2}\Delta C_{\alpha\alpha 22}\frac{\partial^2}{\partial x_1^2}L_{22}(\mathbf{0}) - C_{\alpha\alpha 11}^{0}B'_{1111} - C_{\alpha\alpha 22}^{0}B'_{2211} = -C_{\alpha\alpha 11}^{I}\varepsilon_{1111}^{(T)} - C_{\alpha\alpha 22}^{I}\varepsilon_{2211}^{(T)};\\
&\frac{1}{2}\Delta C_{\alpha\alpha 11}\frac{\partial^2}{\partial x_2^2}L_{11}(\mathbf{0}) + \frac{1}{2}\Delta C_{\alpha\alpha 22}\frac{\partial^2}{\partial x_2^2}L_{22}(\mathbf{0}) - C_{\alpha\alpha 11}^{0}B'_{1122} - C_{\alpha\alpha 22}^{0}B'_{2222} = -C_{\alpha\alpha 11}^{I}\varepsilon_{1122}^{(T)} - C_{\alpha\alpha 22}^{I}\varepsilon_{2222}^{(T)};\\
&\Delta C_{1212}\frac{\partial^2}{\partial x_1\partial x_2}L_{12}(\mathbf{0}) - C_{1212}^{0}B'_{1212} = -C_{1212}^{I}\varepsilon_{1212}^{(T)};
\end{aligned} \tag{2}$$

where

$$\Delta C_{ijkl} = C_{ijkl}^{0} - C_{ijkl}^{I},$$

$$\begin{aligned}
L_{\alpha\beta}(\mathbf{x}) = {} & D_{\alpha\beta 11}(\mathbf{x})B'_{11} + D_{\alpha\beta 22}(\mathbf{x})B'_{22} + D_{\alpha\beta 1111}(\mathbf{x})B'_{1111} + D_{\alpha\beta 1122}(\mathbf{x})B'_{1122} + D_{\alpha\beta 2211}(\mathbf{x})B'_{2211}\\
& + D_{\alpha\beta 2222}(\mathbf{x})B'_{2222} + D_{\alpha\beta 1212}(\mathbf{x})B'_{1212},
\end{aligned}$$

$$B'_{ij} = B_{ij} + \varepsilon_{ij0}^{(T)},$$

$$B'_{ijkl} = B_{ijkl} + \varepsilon^{(\mathrm{T})}_{ijkl} \quad (\alpha, \beta = 1, 2);$$

$\varepsilon^{(\mathrm{T})}_{ij0}$ and $\varepsilon^{(\mathrm{T})}_{ijkl}$ are the constant and quadratic terms in the Taylor series of $\varepsilon^{(\mathrm{T})}_{ij}$, respectively; $D_{ijkl}(\mathbf{x})$ and $D_{ijklmn}(\mathbf{x})$ are the strain fields in an infinite isotropic sheet containing an inclusion with a constant and quadratic eigenstrain, respectively, when the coefficients Bs in Eq. (1) are identity tensors; and the notation $L_{\alpha\beta}(\mathbf{0})$ and $(\partial^2/\partial x_1^2)L_{\alpha\beta}(\mathbf{0})$, etc., means that the Ls and their second derivatives are evaluated at point $(0, 0)$, i.e., the origin of the coordinate system. The tensors Ds in the above equations are also called Eshelby tensors, and they can be evaluated for any polygon-shaped inclusion by using the algorithmic approach outlined in (Rodin, 1996) and (Duong et al., 2001). These detailed evaluations will be omitted here for reason of space.

Once the coefficients B's, thus Bs and ε^*_{ij}, are determined, the elastic fields in the inhomogeinity problem can be obtained from the corresponding results of the equivalent inclusion problem as (Duong et al., 2001):

$$\varepsilon^{\mathrm{I}}_{ij} = D_{ijkl}B_{kl} + D_{ijklmn}B_{klmn}, \tag{3}$$

$$\sigma^{\mathrm{I}}_{ij}(\mathbf{x}) = \begin{cases} C^0_{ijkl}(\varepsilon^{\mathrm{I}}_{kl} - \varepsilon^*_{kl} - \varepsilon^{(\mathrm{T})}_{kl}) & \text{inside } \Omega, \\ C^0_{ijkl}\varepsilon^{\mathrm{I}}_{kl} & \text{outside } \Omega. \end{cases} \tag{4}$$

The stresses in the skin and in the patch inside the reinforced region then can be determined from σ^{I}_{ij} as $C^0_{ijkl}\lfloor(C^{\mathrm{I}}_{klmn})^{-1}\sigma^{\mathrm{I}}_{mn} + \varepsilon^{(\mathrm{T})}_{kl}\rfloor$ and $C^{\mathrm{p}}_{ijkl}\lfloor(C^{\mathrm{I}}_{klmn})^{-1}\sigma^{\mathrm{I}}_{mn} + \varepsilon^{(\mathrm{T})}_{kl} - \varepsilon^{(\mathrm{T})(\mathrm{p})}_{kl}\rfloor$, respectively, where C^{p}_{ijkl} is the patch stiffness, $\varepsilon^{(\mathrm{T})(\mathrm{p})}_{ij}$ is the initial strain in the patch resulting from thermal expansion mismatch between the patch and the repaired skin as defined earlier in the beginning of this section, and C^0_{ijkl} is again the skin stiffness (Duong et al., 2001).

3.2. Stage II analysis

Consider a patched cracked sheet shown in Fig. 1(b) subjected to a crack-surface pressure $p(\zeta)$ which is a negative of the skin normal stress component σ_{yy} found in stage I analysis. The thicknesses of the cracked sheet and the composite patch are small relative to the other in-plane dimensions, so that each component can be considered to be under a generalized plane stress condition with the surface shears transmitted through the adhesive acting as body forces. These body forces are unknowns and only pertinent near the crack. The adhesive layer is treated as a two-dimensional shear spring. This problem is solved by the displacement compatibility method considered earlier by Duong and Yu (1997), and Erdogan and Arin (1972). First, the bonded interfacial area between the patch and the cracked skin is divided into a number of small cells, as shown in Fig. 3. The unknown shear body forces assume to be constant in each cell. Even though the outer boundary of the patch is unbounded in stage II analysis; however, for numerical integration purposes, the bonded interfacial area assumes to be finite and equal to R, and R is chosen such that the stress intensity factor solution does not change appreciably for any larger area. The shear body forces, therefore, have been approximated by a number of discrete forces P_{1i} and P_{2i} distributed uniformly over cells centered at (x_i, y_i).

The interfacial shear body forces P_{1i} and P_{2i} are determined from the displacement compatibility requirement between the cracked sheet and the patch over the bonded interface. The patch–skin displacement compatibility equations in the y-direction are given by:

$$\sum_{m=1}^{M}\left[\sum_{\beta=1}^{2}\left\{v^{P_{\beta m}=1}_{\mathrm{skin}}(x_n, y_n; x_m, y_m) - v^{P_{\beta m}=1}_{\mathrm{patch}}(x_n, y_n; x_m, y_m) - \frac{t_{\mathrm{a}}}{G_{\mathrm{a}}h_m d_m}\delta_{2\beta}\delta_{nm}\right\}P_{\beta m}\right] = -v^{p(\zeta)}_{\mathrm{skin}}(x_n, y_n) \tag{5}$$

for $n = 1, 2, \ldots, M$. In the above equations, M is the number of cells making up the bonded interface; t_{a} and G_{a} are the thickness and shear modulus of the adhesive, respectively; P_{1m} and P_{2m} correspond to the x- and

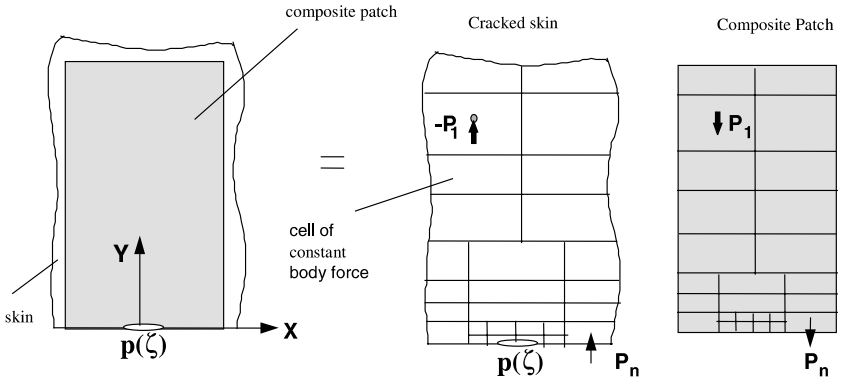

Fig. 3. Free body diagram of a patched cracked sheet under a crack surface pressure $p(\zeta)$. For illustration purpose, $P_1, P_2, \ldots, P_n$ are the y-components of the transmitted shear forces each distributed uniformly over a discretized area (cell) of the bonded interface (Duong and Yu, 1997).

y-components of the interfacial shear body force distributed uniformly over the mth cell centered at (x_m, y_m); h_m and d_m are the length and the width of the mth cell, respectively; $v^{P_{\beta m}=1}(x_n, y_n; x_m, y_m)$ is the y-displacement at the point (x_n, y_n) due to a unit β- (x or y) component of the shear interfacial force acting at (x_m, y_m); $v^{p(\zeta)}_{\text{skin}}(x_n, y_n)$ is the displacement in the skin at (x_n, y_n) due to the crack surface pressure $p(\zeta)$; δ_{ij} is defined similarly to the Kronecker delta which is equal to 0 when $i \neq j$ and 1 when $i = j$. The appropriate expression for $v^{P_{\beta m}=1}(x_n, y_n; x_m, y_m)$ for the cracked skin and the patch, and $v^{p(\zeta)}_{\text{skin}}(x_n, y_n)$ can be found in the reference by Duong and Yu (1997) mentioned above.

Similar equations for the displacement compatibility in the x-direction can also be derived. A total of $2M$ simultaneous equations will result for the determination of $P_{\beta m}$. With the shear body forces known, the total stress intensity factors at each crack tip due to these body forces and due to the crack surface pressure $p(\zeta)$ can be calculated in a straight forward manner as illustrated in the last cited reference.

It should be noted that the present method allows modeling the effects of the pre-existing disbond and the elastic–plastic behavior of the adhesive on the crack tip's stress intensity factor. To account for the former effect, the bonded interfacial area is needed to be discretized in such a way that it will not include any pre-existing disbond region in its domain. For the latter effect, an iterative procedure must be employed in the analysis. For simplicity, the adhesive is modeled in the present work as an elastic–perfectly plastic material. The shear body forces are first assumed to be unknown and the adhesive is assumed to behave linearly elastic. These unknown shear body forces are then determined by solving $2M$ simultaneous equations. If the shear body force per unit area in any cell exceeds the adhesive yield strength, its value will be set to the yield strength and that shear body force will no longer be a sought solution in the next iteration. The coefficient matrix and the right hand side of the $2M$ simultaneous equations are then modified accordingly. In the next iteration, the relative displacement between the skin and the patch per unit adhesive thickness in cells with their shear body force being set to the adhesive yield strength must be checked to see if they are larger than the adhesive yield strain. If not, the prior settings of the values of the body forces in these cells to the adhesive yield strength are incorrect and therefore must be removed. Another iteration is carried out and the whole process is repeated until all prescribed requirements are met.

The solution procedure outlined in this section is general so that it can also be applied to the analysis of an infinite strip patch as well, where the effect of the finite patch width on the stress intensity factor can be properly account for. In that case, appropriate expression for the displacement of a infinite strip patch must be used in Eq. (5). The displacement of an infinite strip patch due to a pair of interfacial shear body forces distributed uniformly over a small cell can also be found in the reference by Duong and Yu (1997).

As a final remark, an alternative approach to stage II analysis had been proposed by Cox and Rose (1994). This approach is based on the crack bridging model, which accounts for delamination in a self consistent manner. This approach yields explicit and accurate analytical estimate for the stress intensity factor.

4. Results and discussion

To assess the accuracy of the present analytical method, a problem of an octagonal patch repair under a uniform low operating temperature is considered. The repair configuration is shown in Fig. 4. The effects of disbond and elastic–plastic adhesive (if any) will be ignored. The material properties of the skin, patch and adhesive as well as the temperature change used in the analysis are given below:

Skin: Aluminum. $E = 72.4$ GPa, $v = 0.33$, $\alpha = 22.5$ μ/°C, $t_s = 1.6$ mm.
Patch: Boron/Epoxy. $E_y = 193.6$ GPa, $E_x = 18.7$ GPa, $v_{yx} = 0.21$, $G_{xy} = 5.5$ GPa, $t_p = 0.79$ mm, $\alpha_y = 4.3$ μ/°C, $\alpha_x = 21.4$ μ/°C.
Adhesive: FM-73. $G = 0.46$ GPa, $t_a = 0.127$ mm.
Temperature change: $\Delta T = -75$ °C.

The sensitivity of the length of the repair cracks relative to the patch width is studied. Four crack lengths of 1.27, 2.54, 3.81, and 5.08 cm are considered in the analysis while the patch geometry is held constant. The thermal stress in the *uncracked* skin underneath the patch and along the line $y = 0$, resulting from stage I analysis, is plotted and compared with the FE solution in Fig. 5. FE results are obtained by using the commercial MSC/NASTRAN code. The skin is modeled as a single layer of solid elements while the patch is modeled as six layers of solid elements, one for each ply. All elements are eight-node isoparametric solid elements. In the finite element model, all nodes at the bottom of the skin surface are restrained from the

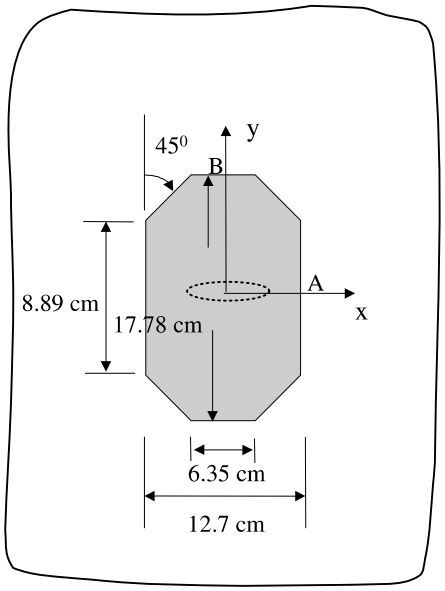

Fig. 4. Geometry of the example problem.

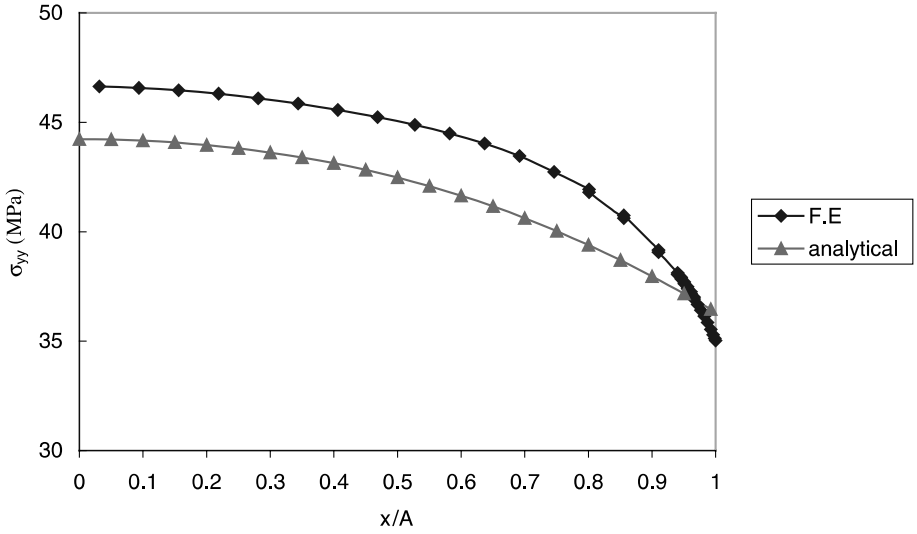

Fig. 5. Thermally induced skin stress σ_{yy} underneath the patch and along the line $y = 0$ for an uncracked patched skin subjected to a uniform temperature change of -75 °C.

out-of-plane displacement. The adhesive is modeled as one layer of anisotropic solids with very small extensional moduli. Stresses from FE analysis are those reported at the centroids of the solid elements and therefore are thickness-average stresses. From Fig. 5, it appears that the analytical result is in general lower than the FE prediction, except near the edge of the patch, and they are in quite good agreement.

The crack tip stress intensity factors evaluated in stage II analysis along with FE results are presented in Table 1. Typical telescopic grids used in the theoretical analysis are given in Fig. 6. FE results are again obtained by using MSC/NASTRAN code with the crack actually being modeled. The skin, patch and adhesive are modeled in a similar manner as for the case without a crack, but with a much finer mesh around the crack. A special 3D crack tip element is used in the NASTRAN analysis to compute the stress intensity factor. This crack-tip element is based on the hybrid assumed stress approach and is compatible with the regular displacement-based elements. Since the skin is modeled as a single layer of solid elements, the stress intensity factor obtained from the finite element analysis is the mid-plane value. From Table 1, results from the two methods are in good agreement within 13%. However, analytical results show a different trend in comparing with the one predicted by the FE method. Several factors might attribute to such discrepancy. First, the analytical method underestimates both the thermal stresses and their gradients in an uncracked skin (see Fig. 5). Secondly, as shown in (Rose, 1988), the stress intensity factor for a patched cracked sheet with a uniform traction acting on the crack surfaces will be nearly constant and thus independent of the crack length when the crack exceeds a certain critical length, providing that there is no edge

Table 1
The stress intensity factors for a cracked skin repaired with an octagonal patch and being subjected a uniform temperature change of -75 °C

Half crack length, a (mm)	Analytical K_I (MPa$\sqrt{m}$)	FE K_I (MPa$\sqrt{m}$)
1.27	3.740	4.304
2.54	3.796	4.298
3.81	3.807	4.214
5.08	3.772	4.024

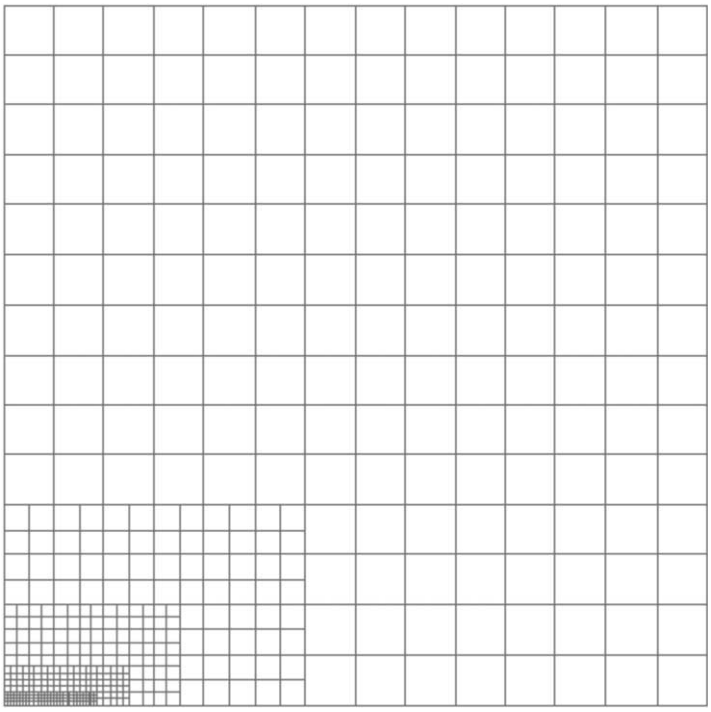

Fig. 6. Typical telescopic grids used in stage II analysis for evaluating the stress intensity factor.

boundary effect. Using the formula given in the reference just mentioned together with appropriate material properties of the present skin, patch and adhesive, this critical crack length is computed to be about 2.5 mm. Since all crack lengths considered here exceed that critical length, the stress intensity factors are therefore expected to be nearly constant and probably (based on intuition) slightly higher for a longer crack in the uniform thermal stress field. This is what we observe from Table 1 for the crack length ratio $a/A < 0.4$. However, since the thermal stress field is a decreasing function of the x-coordinate which is more pronounced for $x/A > 0.4$, K_I may decrease with an increase in crack length for $a/A > 0.4$. Furthermore, since quite different meshes have been employed for different crack lengths in the finite element analyses (the FE models were built using an in-house mesh generator), this mesh's variation will definitely contribute partially to the mentioned discrepancy. For reference, the skin stress near the patch edge at $x = 0$ (point B of Fig. 4) is found to be -35.2 MPa from the two methods.

To assess the effect of these thermal stresses on crack patching efficiency, the above repair problem is reanalyzed for the case of far field mechanical loading only. The far field stress is assumed to be 103.4 MPa, a typical fatigue stress range in transport aircraft fuselage. The stress in the *uncracked* skin along the line $y = 0$, resulting from stage I analysis is plotted in Fig. 7 for comparison with that from the case of thermal loading only. Fig. 7 also includes parallel results from the finite element method. The skin stress near the patch edge at point B is found close to 131 MPa from both methods. The crack tip stress intensity factors evaluated in stage II analysis for the latter case are presented in Table 2. From Tables 1 and 2, one observes that (a) analytical prediction for the mechanical loading case is more accurate than the former case, and (b) the thermal effect on the stress intensity factor can be very significant. For the same repair configuration, the thermal stress intensity factor can be more than 65% of that resulting from the fatigue load. Thus, the effect of thermal stresses is to increase the crack tip stress intensity factor while reducing the load attraction.

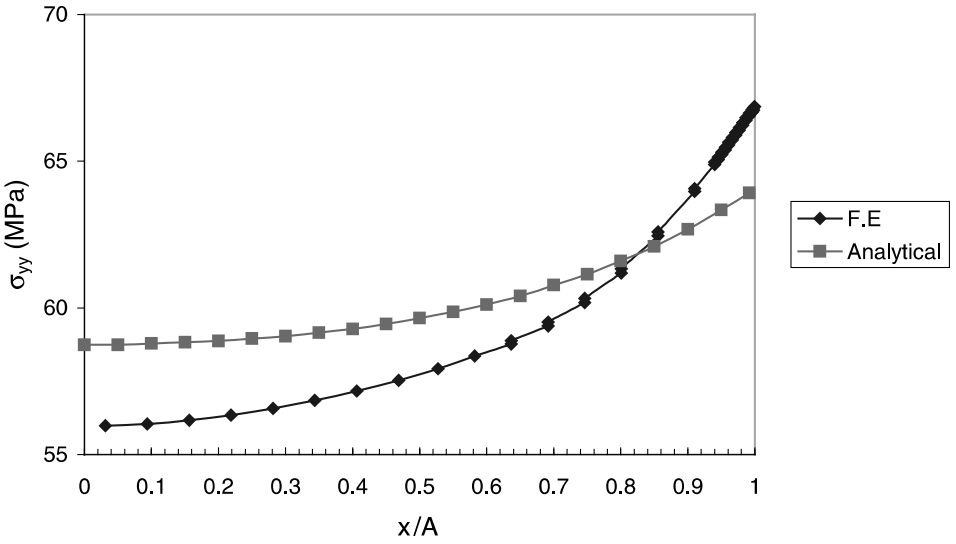

Fig. 7. Skin stress σ_{yy} underneath the patch and along the line $y = 0$ for an uncracked patched skin subjected to a far field stress of 103.4 MPa.

Table 2
The stress intensity factors for a cracked skin repaired with an octagonal patch and being subjected to a far field stress of 103.4 MPa

Half crack length, a (mm)	Analytical K_I (MPa$\sqrt{m}$)	FE K_I (MPa$\sqrt{m}$)
1.27	4.973	5.154
2.54	5.211	5.260
3.81	5.522	5.403
5.08	5.952	5.655

It remains now to show how our curing model using a simplified (step) temperature distribution compares with known analytical results for an isotropic circular patch with a realistic steady state temperature field (Rose, 1988; Wang et al., 2000). This comparison will be illustrated through one specific repair configuration and will be conducted for thermal stresses only. The patch is assumed to be circular and isotropic with the modulus being the same as the principal modulus given in the previous example. The radius of the patch is 12.7 cm. The heating blanket is assumed to be circular. According to our curing model, only the shape of the heating blanket will change thermal stresses but not its size, providing that the blanket is large enough to fully cover the patch. The skin properties are kept the same as before.

In Rose's curing model, the bonded sheet is idealized as a circular plate with a radius of R_0. The circular reinforced region (of radius R_i) of the circular plate is heated to a uniform temperature T_i while the temperature along the plate's edge is prescribed to be T_0. The temperature distribution in the middle region between R_i and R_0 is obtained from the heat transfer theory for a steady state condition. The edge of the plate is also supported by continuous distributed springs with a spring constant of k. To simulate an infinite plate as in our curing model, k had been chosen equal to $(1/(1+\nu)R_0)$ as mentioned in (Wang et al., 2000). Results from Rose's curing model for different R_0 with a free edge condition as well as the case of an infinite plate are compared with our curing model in Table 3 for $T_i - T_0 = -75$ °C. From Table 3, it is clear that our model agree very well with the former model for an infinite plate. For reference, the thermal stresses in the skin and in the patch under uniform temperature curing of the same temperature range are 62.9 and −191 MPa, respectively.

Table 3
A comparison of y-component thermal stresses between Rose's and the present curing model for a circular isotropic patch

R_0/R_i	Rose's model (MPa)		Present model (MPa)	
	σ_s	σ_p	σ_s	σ_p
3	48.8	−140.5	–	–
4	46.4	−136.7	–	–
7	43.6	−131.1	–	–
Infinite plate	36.8	−111.8	36.8	−111.8

5. Conclusion

An analytical method to estimate the thermal effects on crack patching efficiency in a composite bonded repair is presented using Rose's two-stage analysis procedure. Different methods were employed for different stages of the analysis. The problem is formulated under a generalized plane stress condition. The effect of out-of-plane bending is presently ignored; however, it could also be included in the formulation of stage I analysis as previously done by Beom and Earmme (1999) but for an elliptical inhomogeneity and of stage II analysis using a crack bridging model proposed by Wang and Rose (1999).

Appendix A

In this appendix, the material properties of an inhomogeneity that is equivalent to the patched skin are established. As shown in Rose (1981), in the absence of the initial strain in the patch, the material constants of the inhomogeneity are related to those of the patch and the skin by:

$$\begin{aligned} A_x^{\mathrm{I}} &= (A_x^0 t_0 + A_x^{\mathrm{p}} t_{\mathrm{p}})/t_{\mathrm{I}}, \\ A_y^{\mathrm{I}} &= (A_y^0 t_0 + A_y^{\mathrm{p}} t_{\mathrm{p}})/t_{\mathrm{I}}, \\ v_{xy}^{\mathrm{I}} &= (v_{xy}^0 A_y^0 t_0 + v_{xy}^{\mathrm{p}} A_y^{\mathrm{p}} t_{\mathrm{p}})/(A_y^0 t_0 + A_y^{\mathrm{p}} t_{\mathrm{p}}), \\ \mu^{\mathrm{I}} &= (\mu^0 t_0 + \mu^{\mathrm{p}} t_{\mathrm{p}})/t_{\mathrm{I}}, \end{aligned} \tag{A.1}$$

where A_x, A_y, v_{xy} and μ are the material constants which appear in the stress–strain relation for an orthotropic plate as follows:

$$\begin{Bmatrix} \sigma_{11} \\ \sigma_{22} \\ \sigma_{12} \end{Bmatrix} = \begin{bmatrix} A_x & v_{xy}A_y & 0 \\ v_{xy}A_y & A_y & 0 \\ 0 & 0 & \mu \end{bmatrix} \begin{Bmatrix} \varepsilon_{11} \\ \varepsilon_{22} \\ \gamma_{12} \end{Bmatrix}, \tag{A.2}$$

$$A_x \equiv \frac{E_x}{1 - v_{xy}v_{yx}}, \quad A_y \equiv \frac{E_y}{1 - v_{xy}v_{yx}},$$

t is thickness while the superscript or subscripts I, 0 and p signify the inhomogeneity, skin and patch, respectively. For an isotropic plate, $E_x = E_y = E$, $v_{xy} = v_{yx} = v$, and $\mu = E/2(1 + v)$.

In the case the patch is subjected to a prescribed initial strain $\varepsilon_{ij}^{(\mathrm{T})(\mathrm{p})}$, it very easy to show that the constitutive relation for the equivalent inhomogeneity is given by:

$$\begin{aligned} \sigma_{ij}^{\mathrm{I}} &= C_{ijkl}^{\mathrm{I}}(\varepsilon_{kl} - \varepsilon_{kl}^{(\mathrm{T})}), \\ \varepsilon_{ij}^{(\mathrm{T})} &= \frac{t_{\mathrm{p}}}{t_0} C_{ijkl}^{\mathrm{I}-1} C_{klmn}^{\mathrm{p}} \varepsilon_{mn}^{(\mathrm{T})(\mathrm{p})}, \end{aligned} \tag{A.3}$$

where C_{ijkl} is the stiffness, which in matrix form is given by Eq. (A.2) above.

References

Beom, H.G., Earmme, Y.Y., 1999. The elastic field of an elliptic cylindrical inclusion in a laminate with multiple isotropic layers. Journal of Applied Mechanics 66, 165–171.

Cox, B.N., Rose, L.R.F., 1994. Time- or cycle dependent crack bridging. Mechanics of Materials 19, 39–57.

Duong, C.N., Wang, J.J., Yu, J., 2001. An approximate algorithmic solution for the elastic fields in bonded patched sheets. International Journal of Solids and Structures 38, 4685–4699.

Duong, C.N., Yu, J., 1997. The stress intensity factor for a cracked stiffened sheet repaired with an adhesively bonded composite patch. International Journal of Fracture 84, 37–60.

Duong, C., Knauss, W.G., 1995. A nonlinear thermoviscoelastic stress and fracture analysis of an adhesive bond. Journal of Mechanics and Physics of Solids 43, 1505–1549.

Erdogan, F., Arin, K., 1972. A sandwich plate with a part-through and a debonding crack. Engineering Fracture Mechanics 4, 449–458.

Freddell, R.S., 1994. Damage Tolerant Repair Techniques for Pressurized Aircraft Fuselages, Ph.D. Thesis, Delft Technical University, Netherlands.

Rodin, G.J., 1996. Eshelby's inclusion problem for polygons and polyhedra. Journal of Mechanics and Physics of Solids 44, 1977–1995.

Rose, L.R.F., 1981. An application of the inclusion analogy. International Journal of Solids and Structures 17, 827–838.

Rose, L.R.F., 1988. Theoretical analysis of crack patching. In: Baker, A.A., Jones, R. (Eds.), Bonded Repair of Aircraft Structures. Kluwer Academic Publisher.

Wang, C.H. et al., 2000. Thermal stresses in a plate with a circular reinforcement. International Journal of Solids and Structures 37, 4577–4599.

Wang, C.H., Rose, L.R.F., 1999. A crack bridging model for bonded plates subjected to tension and bending. International Journal of Solids and Structures 36, 1985–2014.